Electronic Supplementary Material (ESI) for Journal of Materials Chemistry C.

Supporting Information

Effects of Solution Processable CuI Thin Films with Al_2O_3-Based Sandwiched Architecture for High-Performance p-Type Transistor Applications

Hyun-Ah Lee,[a] Tae In Kim,[b] Hyuck-In Kwon,[*a] and Ick-Joon Park[*c]

[a]Department of Intelligent Semiconductor Engineering
Chung-Ang University
Seoul, Korea 06974

[b]Department of Electrical Engineering
Inha University
Incheon, Korea 22212

[c]Department of Electrical and Electronic Engineering
Joongbu University
Goyang, Korea 10279

Corresponding authors:
[*] Prof. H.-I. Kwon : hyuckin@cau.ac.kr
[*] Prof. I.-J. Park : ickjoon.park@joongbu.ac.kr

S1. Ellipsometry spectra of the Al_2O_3 interfacial layers.

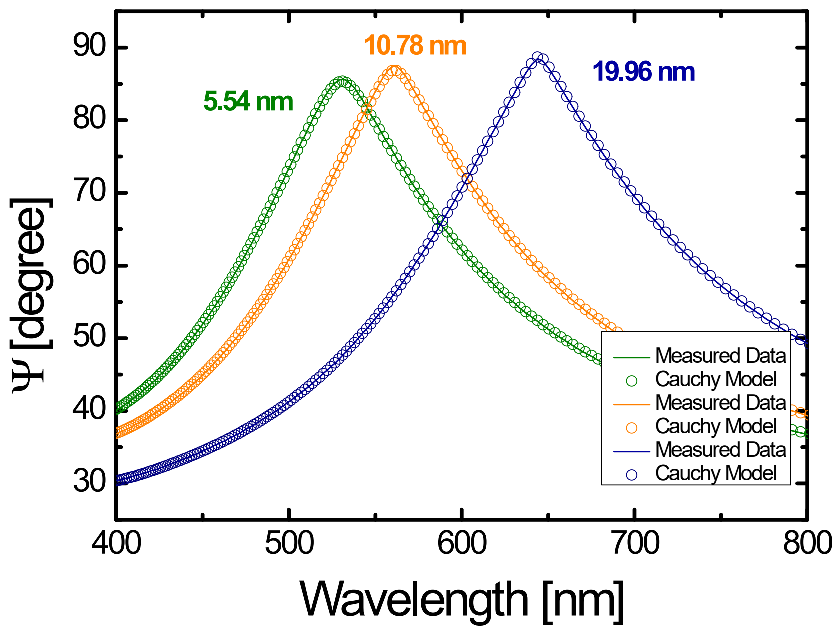

Figure S1. Thicknesses of the Al_2O_3 interfacial layers measured by spectroscopic ellipsometry.

.

S2. Transfer curves of the CuI TFTs without Al_2O_3 passivation layer.

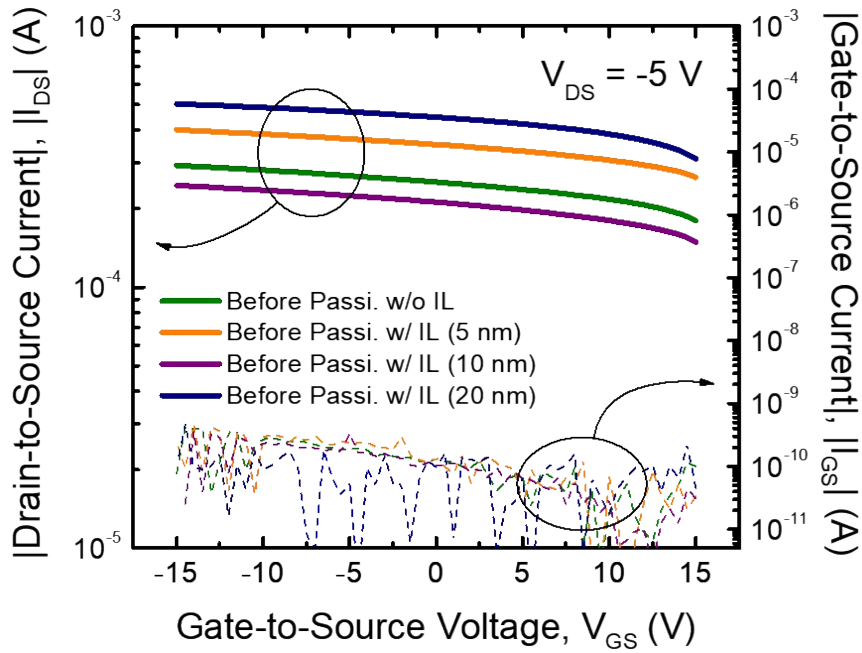

Figure S2. Transfer curves of the CuI TFTs with the Al_2O_3 interfacial layers having various thicknesses of 0 to 20 nm without passivation layer.

S3. Dual-sweep transfer curves of the CuI TFTs with various Al_2O_3-based sandwiched architectures.

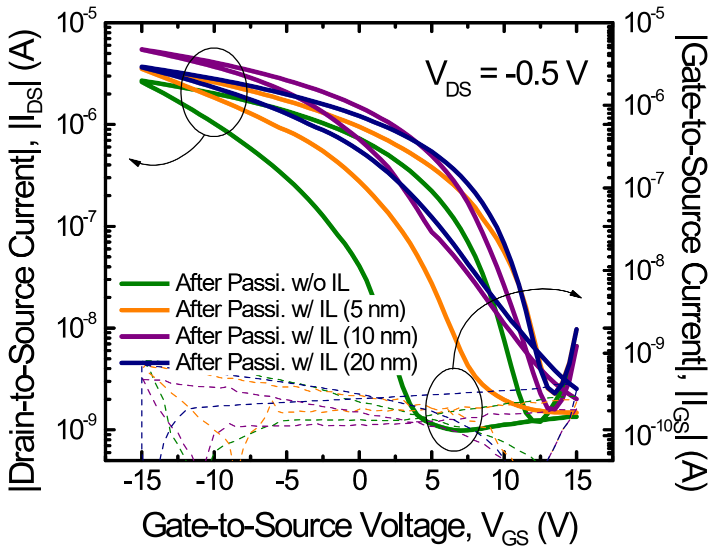

Figure S3. Dual-sweep transfer curves of the CuI TFTs with various Al_2O_3-based sandwiched architectures having thicknesses of 5 to 20 nm.

S4. AFM topographies of various gate dielectric stacks.

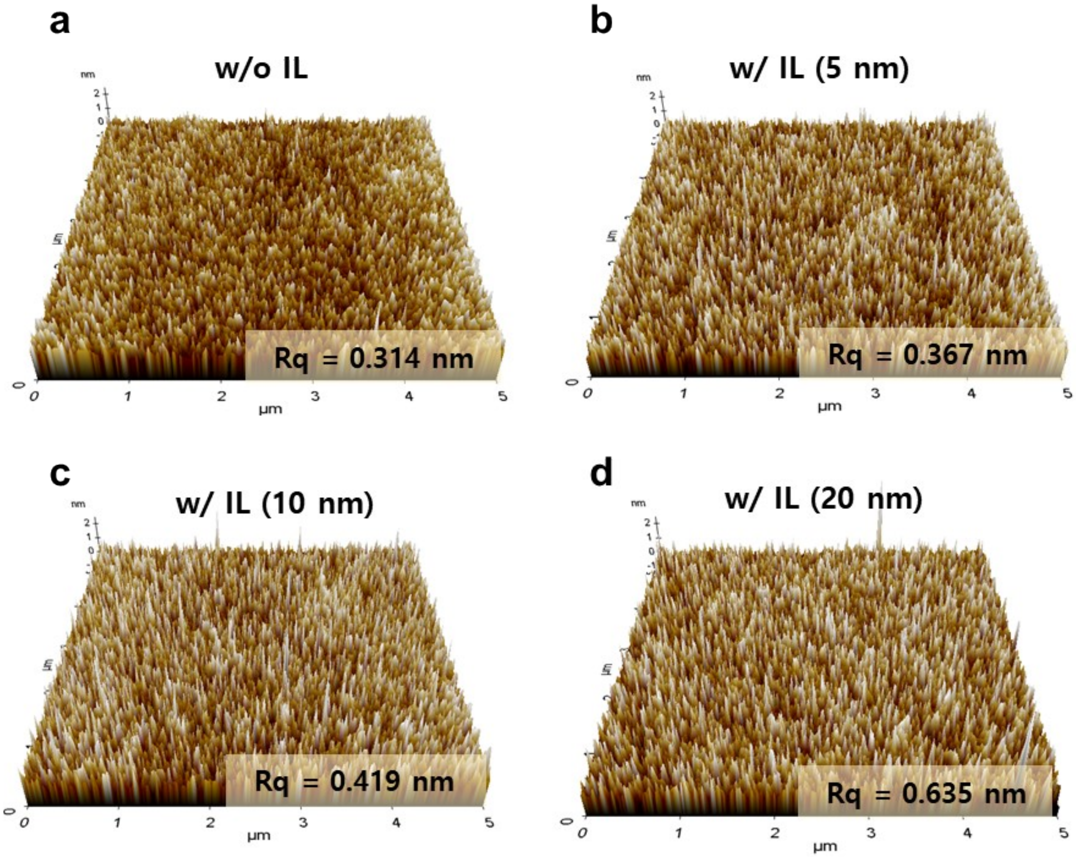

Figure S4. AFM topographies of various gate dielectric stacks (a) without the Al_2O_3 interfacial layer and with the Al_2O_3 interfacial layer having thicknesses of (b) 5 nm, (c) 10 nm, and (d) 20 nm.

S5. SEM images of the CuI thin film with the Al_2O_3-based sandwiched architecture.

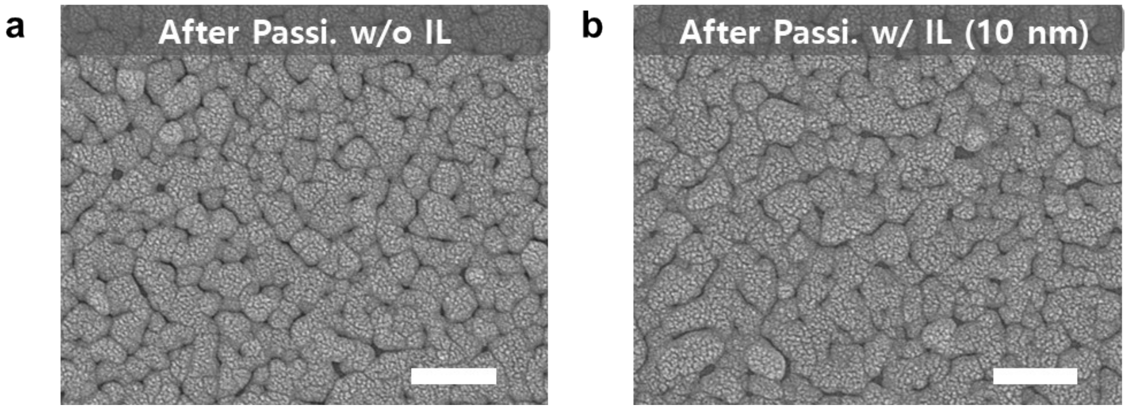

Figure S5. SEM images of the CuI thin film with the Al_2O_3-based sandwiched architecture (a) without Al_2O_3 interfacial layer and (b) with 10 nm-thick-Al_2O_3 interfacial layer. The scale bar represents 100 nm.

S6. Output curves of the CuI TFTs with Al_2O_3-based sandwiched architecture.

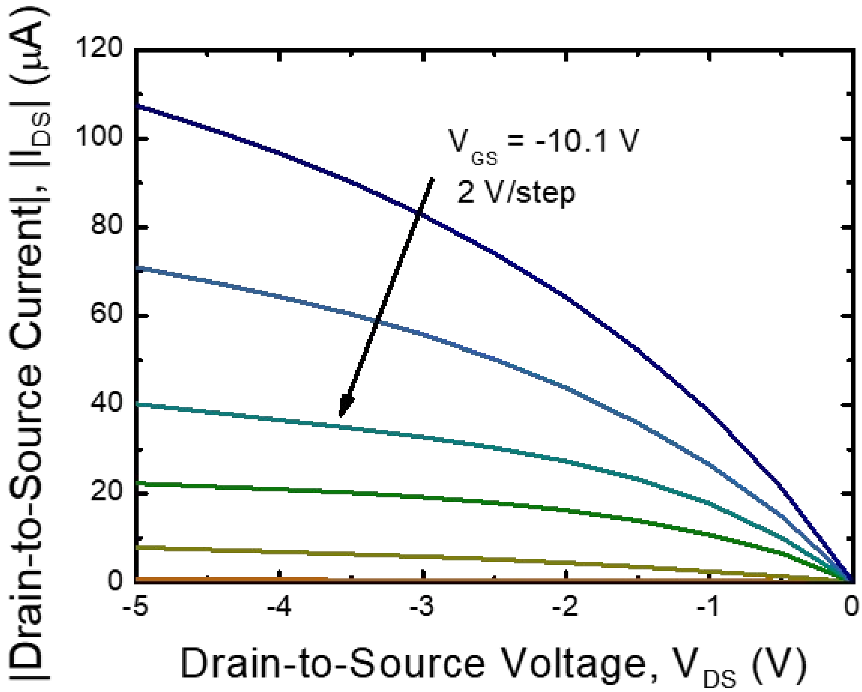

Figure S6. Output curves of the CuI TFTs with Al_2O_3-based sandwiched architecture.

S7. Transfer curves ($\sqrt{I_{DS}}$ versus V_{GS}) of the CuI TFTs.

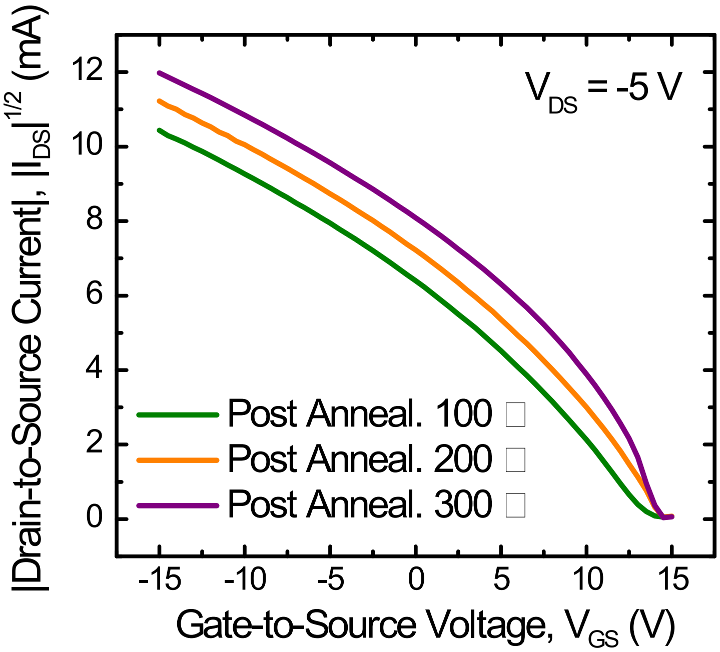

Figure S7. Transfer curves ($\sqrt{I_{DS}}$ versus V_{GS}) of the CuI TFTs after post annealing process.

S8. Transfer curves of the CuI TFTs before and after thermal annealing.

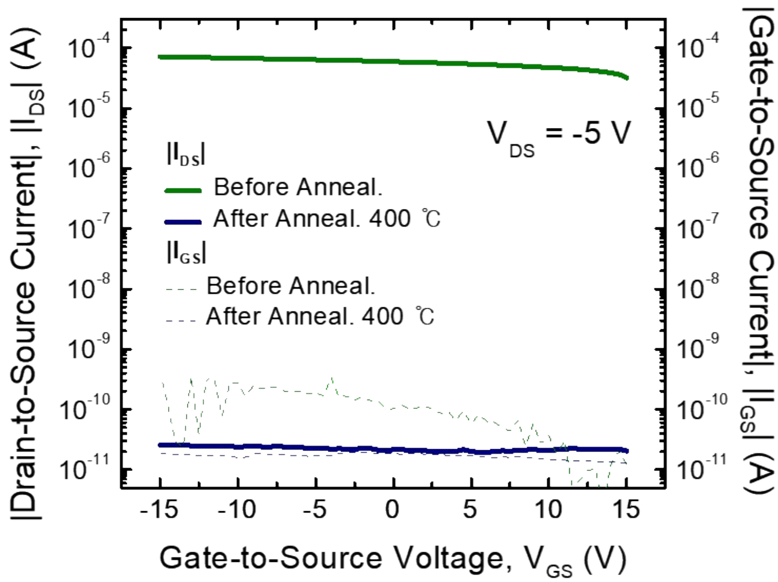

Figure S8. Transfer curves of the CuI TFTs before and after thermal annealing at a temperature of 400 °C.